Silvio Francisco Brunatto
brunatto@ufpr.br
Departamento de Engenharia Mecânica
Universidade Federal do Paraná (UFPR)
81531-990 Curitiba, PR, Brazil

Plasma Assisted Parts' Manufacturing: Sintering and Surface Texturing – Part II – Influence of Inter-Cathode Distance and Gas Pressure

The acquirements and potentiality universe of cleaning, heating and/or sputtering effects caused by plasma species bombardment phenomenon on the surface characteristics and finishing of manufactured parts treated in DC abnormal glow discharge opens a new research and development field, called here of Plasma Assisted Parts' Manufacturing (PAP'M). The adequate control of the sputtering mechanism allows the obtainment of different kinds of surface. Therefore, the design of rough or smooth surface, presenting a modified distribution of surface porosity and texturing could be idealized, in accordance with the desired surface characteristics, as the parts are simultaneously sintered and treated. This is the second part (out of two) of the work performed in hollow cathode discharge (HCD) and it presents the first results of the surface morphology's changes in the pressed iron samples and in the internal surface of the external cathode as a function of the inter-cathode distance and gas pressure. Potential applications include small diameters' cylindrical parts and components like axles, pins, pivots, and tubes and pipes presenting small internal diameters. Sputtering effects were quantified by means of mass loss, and Ra and Rz roughness measurements and qualified by means of SEM. Results indicate the sputtering mechanism is highly dependent of the hollow cathode effect, in HCD sintering and surface texturing treatments, comprising an important contribution to the development of green technologies for surface texturing, surface engineering, and part's manufacturing.
***Keywords**: Plasma Assisted Parts' Manufacturing (PAP'M), Hollow Cathode Discharge (HCD), plasma sintering, surface texturing, sputtering, inter-cathode distance, gas pressure*

Introduction

As presented in Part I, the metallic parts processed by means of DC abnormal glow discharge (Chapman, 1980; Muzart et al., 1997) and hollow cathode discharge (HCD) present characteristics that are directly related to the cleaning, heating and/or sputtering effects caused by plasma species (ions and neutrals) bombardment phenomenon (v. Engel, 1994; Koch et al., 1991; Kolobov and Tsendin, 1995; Benda et al., 1997; Koch et al., 1991; Brunatto et al., 2005; Brunatto and Muzart, 2007; Brunatto et al., 2008). In addition, the acquirements and potentiality universe of these effects on the manufactured parts' surface characteristics are far-away from being finished. So, a new research and development field could be evidenced, which is called here of Plasma Assisted Parts' Manufacturing (PAP'M). Considering the adequate control of the sputtering mechanism can allow the obtainment of different kinds of surface, the design of rough or smooth surface presenting a modified distribution of surface porosity could be idealized, in accordance with the desired surface characteristics.

In this study (Part II) performed in hollow cathode discharge (HCD), results of the surface morphology's changes in the cylindrical pressed iron samples and in the internal surface of the external cathode are presented as a function of the inter-cathode distance and gas pressure. Special attention is given for both the parameters, which tend to be the principal parameters in HCD. This affirmation is based on the fact that HCD occurs in cathodes presenting cavities or hollows, when the discharge fills the cavity under given conditions governed by the "a x p" product (a: inter-cathode distance; and p: gas pressure). In practice, considering the possible geometries and arrangements, the hollow cathode effect occurs for "a x p" products ranging from 0.375 to 3.75 cmTorr (Koch et al., 1991).

Two aspects were studied: a) the superficial pores' morphology modification in pressed samples processed by HCD, which could be explored as a new way to perform sintering and surface texturing treatments in cylindrical parts like axles, pins, and pivots presenting small diameters (the study of the chemical composition modification of the iron sample's surface is not considered here, since it is presented in previous work, Brunatto et al., 2001); and b) in the internal surface of the external cathode, which acts as a pipe (see Fig. 1), the mechanism of the metallic atoms deposition, altering its start chemical composition and the surface morphology via HCD, which could be explored as a new way to perform deposition and surface texturing treatments in pipes presenting small internal diameters. Sputtering effects are quantified by means of mass loss measurements and qualified by means of SEM. Measurements of roughness are presented too. The overall work comprises the study of different parameters, including the influence of sintering time and sintering temperature (Part I), and inter-cathode distance and gas pressure (Part II), indicating the sputtering mechanism could be adequately controlled to attend the premise, comprising an important contribution to the development of green technologies for surface texturing, surface engineering, and consequently for part's manufacturing.

Nomenclature

Ar = *argon*
DC = *Direct Current*
E.C. = *external cathode*
HCD = *Hollow Cathode Discharge*
H_2 = *hydrogen*
PAP'M = *Plasma Assisted Parts' Manufacturing*
SEM = *Scanning Electron Microscopy*
ton = *switched-on pulse time*

Paper accepted December, 2009. Technical Editor: Anselmo Eduardo Diniz

a = *inter-cathode distance*
p = *gas pressure*
Ra = *roughness Ra*
Rz = *roughness Rz*
ΔT = *temperature increment*

Experimental Procedure

Figure 1 shows an "in situ" view of the plant in use showing the hollow cathode discharge and both the cathodes. Detailed representation of the experimental apparatus is available in the earlier reports (Brunatto et al., 2001; Brunatto and Muzart, 2007).

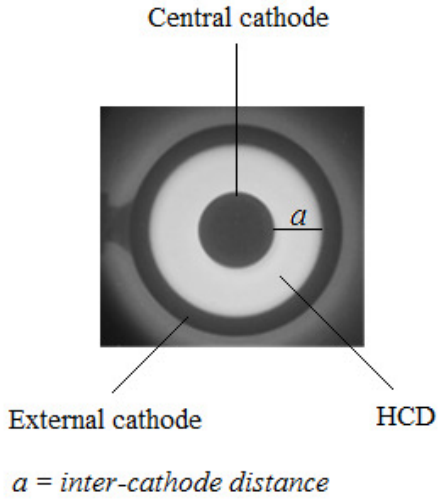

Figure 1. An "in situ" view of the plant in use showing the hollow cathode discharge and both the cathodes.

The discharge chamber consisted of a 350 mm diameter, 380 mm high stainless steel cylinder attached to steel plates and sealed with o-rings at both ends. The system was evacuated to a residual pressure of 1.33 Pa using a two stage mechanical pump. The gas mixture of Ar and H_2 was adjusted by two mass flow controllers of 8.33×10^{-6} and 3.33×10^{-6} m^3s^{-1} operating at full scale, for Ar and H_2 gas, respectively. The pressure in the vacuum chamber was adjusted with a manual valve and measured with a capacitance manometer of 1.33×10^3 Pa (10 Torr) in full-scale operation.

A sample of 9.5 mm diameter and 10 mm height was placed on an AISI 1008 carbon steel support (12 mm height) that served as the central cathode. A cylindrical low carbon steel part (3.5 mm height) was placed at the top of the sample in order to generate a homogeneous annular discharge. The external cathodes were machined from an AISI 310 stainless steel tube (atomic % composition: 25.0% Cr, 16.0% Ni, 1.5% Mn, 1.5% Si, 0.03% C and the balance, Fe) to internal diameters of 15.9, 21.2, and 27.9 mm, 2 mm wall thickness and 25.4 mm height. The internal surfaces of the external cathodes were hand finished by polishing using 1200 grade sand-paper in high rotation machine.

Both cathodes were negatively biased at the same voltage, using a square form pulsed power supply. The voltage was set to 565 V. To ensure a stable discharge, an electrical resistance was connected in series between the power supply and the discharge chamber. The power transferred to the plasma was adjusted by varying the time that the pulse was switched on (ton). The pulse period used was 200 μs. The temperature of the sample was selected by adjusting the on/off time of the pulsed voltage. For the inter-cathode distance study the ton values applied to the cathodes to obtain 1423 K (1150 °C) were 24, 39 and 65 μs (these values correspond to the average of the last 20 min at the sintering stage), and the central cathode current and the total current (central cathode plus external cathode current) were 162, 157 and 154 mA and 404, 451 and 532 mA, for inter-cathode distances of 3.2, 5.8 and 9.2 mm, respectively. For the pressure study, the ton values applied to the cathodes to obtain 1423 K (1150 °C) were 77, 41, 37 and 59 μs (these values correspond to the average of the last 20 min at the sintering stage), and the central cathode current and the total current (central cathode plus external cathode current) were 138, 159, 161 and 184 mA and 363, 458, 554 and 770 mA, for pressures of 133, 400, 800 and 1200 Pa (1, 3, 6 and 9 Torr), respectively. The temperature was measured by means of a chromel–alumel (type K of 1.5 mm diameter) thermocouple inserted to a depth of 8 mm into the sample holder.

Samples of unalloyed iron were produced using Ancorsteel 1000C iron powder (99.75 wt% pure). A double action press with moving die body was used to press the samples that had a green density of 7.0 ± 0.1 gcm^{-3}. The mass of the pressed samples was typically around 5.0 g. The mass loss of the samples was measured with a 0.1 mg precision balance.

Sintering was performed at 1423 K (1150 °C) for inter-cathode distances of 3.2, 5.8 and 9.2 mm, and time of 120 min, pressure of 400 Pa (3 Torr), with a gas flow of 5×10^{-6} m^3s^{-1} (in accordance with Brunatto and Muzart, 2007), and a gas mixture composed of 80% Ar and 20% H_2. The same was applied to the sintering at pressures of 133, 400, 800 and 1200 Pa (1, 3, 6 and 9 Torr), for time of 60 min and inter-cathode distance of 5.8 mm. The sintering procedure was divided into three steps:

a) The samples were cleaned under a discharge at 723 K (450 °C) for 30 min, using 133 Pa (1 Torr) pressure and the resistance adjusted to 100 Ω;

b) They were heated at a heating rate of 0.42 Ks^{-1} (0.42 $°Cs^{-1}$) and sintered at specified temperature, using 400 Pa (3 Torr) pressure and resistance adjusted to 50 Ω;

c) The samples were cooled under a gas mixture flow.

Characterization was carried out on the sample's cylindrical surface and on the internal cylindrical surface of the external cathode, which are the surfaces exposed to the exponential glow discharge. The surface morphology of the samples was characterized by means of scanning electron microscopy, using a Philips XL-30 microscope. The chemical composition of the surfaces was obtained by means of energy dispersive x-ray microprobe analysis. Sputtering effects were quantified by means of mass loss and roughness determination. Measurements of roughness were conducted in accordance with ISO 4287 (1997) for Ra and Rz determination, using Mahr (Concept) equipment, filter Gauss, and 400 μm measurement length and 80 μm wave length (five divisions) for the sintered samples, and 4 mm measurement length and 0.80 mm wave length (five divisions) for the internal surfaces of the external cathode. Mathematically, Ra is the arithmetic average value of the profile departure from the mean line within a sampling length and is given by the sum of the absolute values of all the areas above and below the mean line divided by the sampling length. Otherwise, Rz is the maximum height of profile (peak to valley) within a sampling length, and is usually analyzed as an average of the 5 values comprising the highest value for peak to valley distance taken in each division in the sampling length.

Results and Discussion

Characterization of the Hollow Cathode Discharge

In order to evaluate the influence of the hollow cathode configuration on the heating process, Fig. 2(a) presents the variation of the sample temperature (central cathode) as a function of inter-

cathode distance (a = 3.2, 5.8 and 9.2 mm) and pressure (ranging from 80 to 800 Pa, or 0.6 to 6 Torr), for a fixed condition of 40 μs ton, 470 ± 5 V voltage (without the presence of an electrical resistance), and 2 x 10^{-6} m^3s^{-1} gas flow. And Fig. (2b) presents the temperature increment by hollow cathode effect (ΔT) which was calculated by the difference of the temperatures measured in two different conditions: a) in HCD configuration, for different inter-cathode distances; and b) in linear glow discharge configuration (condition obtained without external cathode – see Fig. 2a).

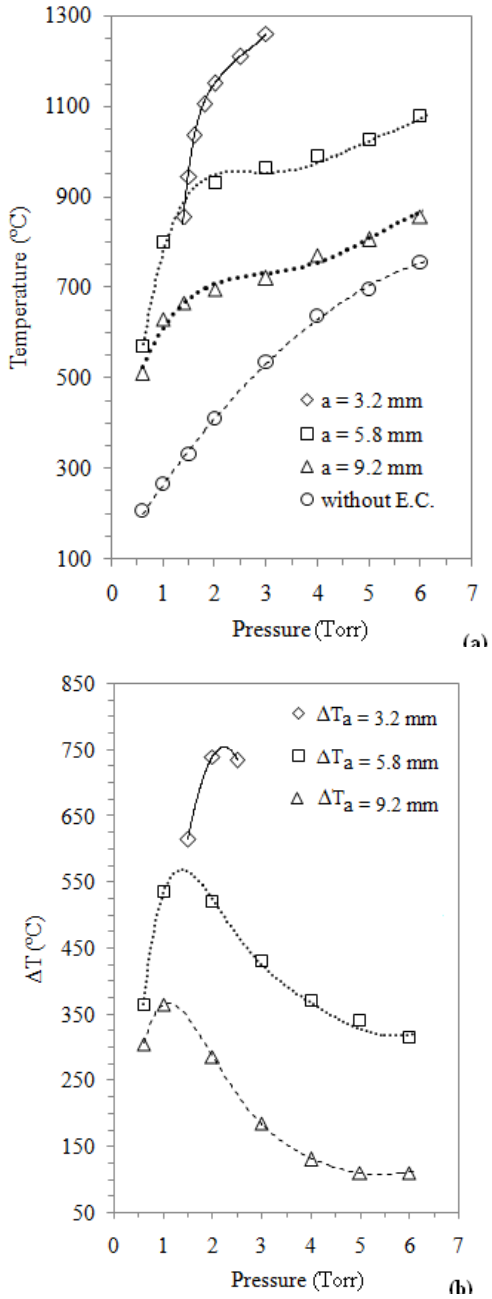

Figure 2. (a) Variation of the sample temperature; and (b) variation of the temperature increment (ΔT) as a function of hollow cathode effect for different inter-cathode distance and pressure, for a fixed condition of 40 μs ton, 470 ± 5 V voltage, and 2 x 10-6 m^3s^{-1} gas flow.

In accordance with Fig. 2(a), significant increase of temperature was observed in the hollow configuration as compared to the linear abnormal glow discharge; the higher the confinement of the hollow cathode configuration, the more accentuated was the increase of temperature. Results indicate there is a range of pressure from 1 to 3 Torr that optimize the hollow cathode effect. At the pressure of 400 Pa (3 Torr) and the inter-cathode distance of 3.2, 5.8 and 9.2 mm, temperatures of 1533, 1238 and 993 K (1260, 965 and 720 °C) were obtained, respectively. When the distance is 3.2 mm, the discharge is confined in such a way that the ionization increase is excessively high, as discussed by von Engel (1994). As a consequence, for inter-cathode distance of 3.2 mm and pressures equal or higher than 1.4 Torr, the current density and thus the temperature increased rapidly, which makes it very hard to achieve accurate temperature values.

It is important to emphasize that an unstable annular glow discharge was verified for p = 133 Pa (1 Torr) and a = 3.2 mm condition, resulting in "a x p" product of 0.32 cmTorr. Note that this value is smaller than 0.375 cmTorr and is in agreement with the practice rule for "a x p" product (Koch et al., 1991), as previously mentioned. In addition, it is interesting to observe (see in Fig. 2(a) the data indicated as without E.C.) that the optimization of the central cathode's temperature increment in relation to the linear glow discharge tends to occur for a value of "a x p" product roughly constant, on the order of 0.90 cmTorr (0.32 cm x 2.7 Torr, 0.58 cm x 1.5 Torr, and 0.92 cm x 1.0 Torr, or 0.86, 0.87, and 0.92 cmTorr, for inter-cathode distances of 3.2, 5.8 and 9.2 mm, respectively). Finally, it is evidenced a tendency of decreasing the central cathode's temperature increment as the pressure is increased. An example of it is verified for inter-cathode distance of 9.2 mm and pressures higher than 5.0 Torr, resulting in "a x p" products higher than 3.75 cmTorr.

As discussed by v. Engel (1994), for "a x p" products values higher than 3.75 cmTorr the glow region of each cathode wall tends to separate and to act as two independent linear glow discharges, which explain the decreasing of the hollow cathode effect. Otherwise, for "a x p" products values smaller than 0.375 cmTorr, there is not sufficient space for the region luminescent to form, and the discharge becomes unstable (v. Engel, 1994).

The above mentioned results can also be observed considering the temperature increment by hollow cathode effect (ΔT) shown in Fig. 2(b), which clearly indicate the related effect is optimized for pressures ranging from 1 to 3 Torr and smaller inter-cathode distances, and it is decreased for higher pressures. As an example, for conditions of a = 5.8 mm and pressures higher than 6 Torr, the temperature gain by the hollow cathode effect tends to a minimum, and consequently the central cathode's temperature increment (ΔT) tends to a constant value.

Finally, the effect of the pressure on the sputtering mechanism must be explained. The higher the pressure, the higher is the neutrals density (Ar atoms and H_2 molecules) in the discharge. In such case, the mean free path is strongly reduced and the energy transferred to the ions crossing the cathode sheath is considerably diminished (Chapman, 1984), since a higher amount of collisions between the plasma species could be expected. Consequently, the incident ions and neutrals impact on the cathode's surface with lower energy, implying in a reduction of the sputtering effect in both the cathodes.

Aspects Related to the Inter-Cathode Distance

a) In the Cylindrical Surface of the Iron Samples

Surface finishing aspects of the iron samples sintered in HCD are shown in Fig. 3. To emphasize the effects of the ion bombardment on the surface characteristics of the samples, a same place was characterized by SEM before (in the pressed or green

state – Fig. 3: a1, b1, and c1) and after plasma exposition (in the sintered state – Fig 3: a2, b2, and c2) for inter-cathode distances of 3.2, 5.8 and 9.2 mm, respectively.

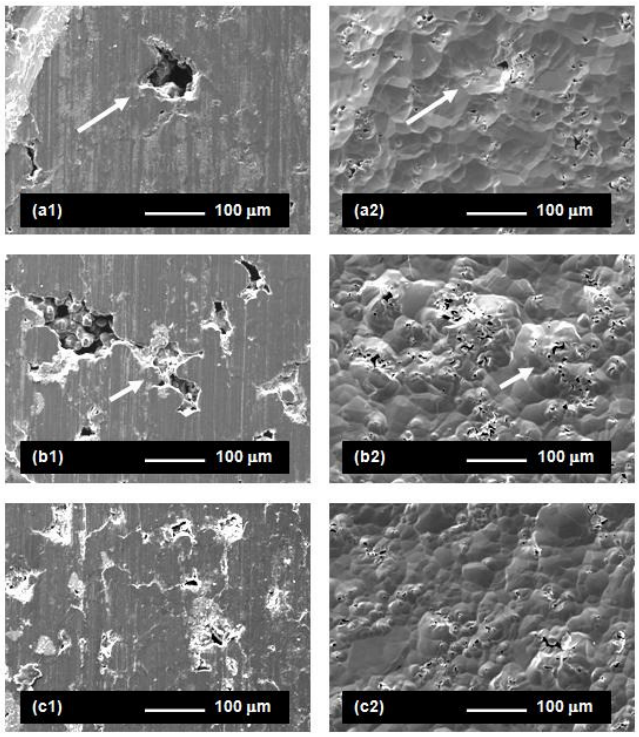

Figure 3. Surface finish aspects of the iron samples: a1, b1, and c1) in the pressed state; and a2, b2, and c2) after plasma exposition, for inter-cathode distance of 3.2, 5.8, and 9.2 mm, respectively.

Two different aspects can be observed: a) the surface finishing modification; and b) the surface pores' morphology modification. The first aspect is related to the confrontation of the results shown in Fig. 3 (a1 x a2, b1 x b2, c1 x c2), which indicates strong modification of the surface finishing occurring after HCD processing. The changes in the surface finishing can be explained by the intense sputtering mechanism caused by ion bombardment phenomenon on the samples' surface exposed to the plasma in the HCD, resulting in the sputtering of iron atoms from the sample surface. Despite the fact that significant surface finishing differences were verified between the pressed and sintered samples, the effect of the inter-cathode distance on the surface finishing (Fig. 3: a2, b2, c2) was not so evident (as will be discussed in the results presented in Figs. 4 and 5). This fact is probably associated to the long sintering time (of 120 min), resulting in a long exposition of the surface to an ion bombardment under the hollow cathode condition, which tends to reduce the differences on surface morphology, for the discharge parameter studied.

Figure 4 shows the mass loss measurements of the samples, taken to evaluate the sputtering effect on the central cathode according to the inter-cathode distance. The mass losses were 0.97, 0.65 and 0.42% (50, 32 and 22 mg) for inter-cathode distances of 3.2, 5.8 and 9.2 mm, respectively. The data shown in Fig. 4 comprising the mass loss (y), given in % unit, were mathematically treated to estimate the mass losses for different inter-cathode distances (x), given in mm unit. The equation of the fitted curve, resulting in an exponential approach was:

$$y = 1.491\, e^{-0.13x} \qquad (R^2 = 0.997) \qquad (1)$$

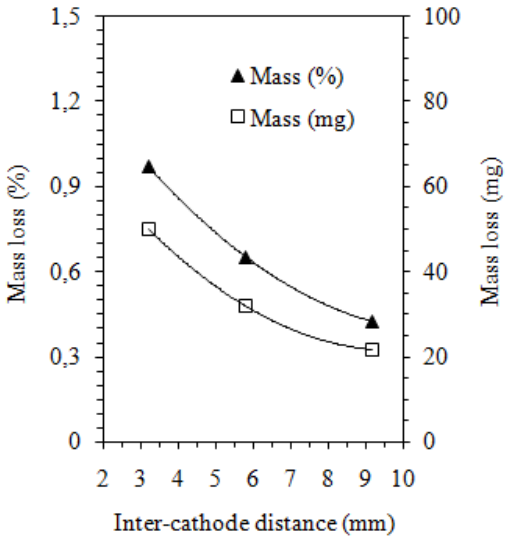

Figure 4. Mass loss measurements of the iron samples processed for different inter-cathode distances.

Interesting to emphasize that the higher mass loss values were obtained to smaller ton values applied to the cathodes, as presented in the experimental procedure. This result agrees with the expected for hollow cathode, since both the heating and the sputtering effects tend to be stronger for smaller inter-cathode distance, as discussed in Fig. 2.

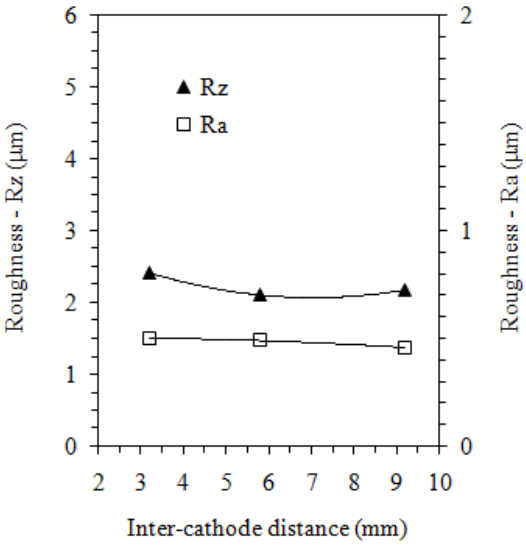

Figure 5. Ra and Rz roughness measurements of the iron samples processed for different inter-cathode distances.

Figure 5 shows the Ra and Rz roughness measurements of the samples, taken to evaluate the surface changes as a consequence of the sputtering effects on the central cathode, according to the inter-cathode distance. The Ra and Rz values were 0.50, 0.49 and 0.46 µm, and 2.4, 2.1 and 2.2 µm for inter-cathode distances of 3.2, 5.8 and 9.2 mm, respectively, indicating a slight decrease of the roughness occurred as a function of the inter-cathode distance, despite the strong surface finishing's modification verified, as shown in Fig. 3 (a1 x a2, b1 x b2, c1 x c2). The above result could indicate that the probability of incident ions' collision occurring in

a random position of the sample surface tends to be the same, independently if the collision occurs in a peak or in a valley position of the plasma exposed surface, which would explain the similar results obtained for the roughness, as a consequence of the sputtering.

The second aspect is related to the fact that the sputtering effect tends to promote changes on the superficial pores' morphology, considering the start pores existent in the pressed samples cylindrical surfaces (Fig. 3: a1 x a2, b1 x b2, c1 x c2). Strong modifications in the surface finishing and in the open pore apparent volume can be observed for the samples processed for different inter-cathode distances. Note that the 3.2 mm inter-cathode distance processed sample presents in its pressed state (Fig. 3: a1) an open and large superficial pore, which was practically closed after processing (Fig. 3: a2). It should be noted that alteration of the superficial pores' morphology was congruent with the mass loss measurements, being dependent on the parameter "a", as verified for the other conditions presented in Fig. 3 (b1 x b2, c1 x c2). In addition, the open pores tend to become closed as a consequence of the intense material transport mechanism verified for the metallic atoms, by the interactions in the plasma-surface system. So, a tendency of more efficient surface modification in the pore size distribution could be expected by decrease of the inter-cathode distance, which would lead to a fine and disperse distribution of open small pores, as a consequence of the sputtering mechanism enhancement. This result should be emphasized, since it confirms that the success in closing open pores is strongly dependent on the start pore size, besides the electrical discharge parameters. The above findings indicate that the inter-cathode distance is an important discharge parameter, when reduction in the superficial pore size is desirable. The results presented here indicate that the hollow cathode discharge could be applied to develop a new green technology for surface texturing, becoming a new technique to improve surface properties such as roughness and morphology. These properties are significant parameters for many applications directly related to the coatings adhesion, tribological performance, and others, according to Gupta et al. (2007), Basnyat et al. (2008), and Krupka et al. (2008).

b) In the Internal Surface of the External Cathodes

Surface finish aspects of the internal surface of the external cathodes processed in HCD are shown in Fig. 6. To emphasize the effects of the sputtering on the characteristics of the internal surface as a function of the inter-cathode distance, results are compared with the start surface condition (Fig. 6d), which was obtained by polishing. The results indicate the surface morphology is strongly modified. A textured surface can be observed for the largest inter-cathode distance condition (a = 9.2 mm, Fig. 6c). The surface is characterized by the presence of grown micrometer particles. It is to be noted that the surface texturing obtained here (Fig. 6c) is similar to that verified for 60 min sintering time and a = 5.8 mm condition, as previously shown in Part I, which also confirms the assumption of the obtainment of a sintered deposit layer with a typical morphology of powder particles, in accordance with the work of Romanowsky and Wronikowsky (1992), and subsequent enlargement. In addition, the enlargement of the round particles could be associated to the particles coalescence phenomenon, as a consequence of the intense superficial diffusion, which would be activated by the ion bombardment effect, allied to the decrease of the surface free energy variation. The above result is in accordance with the expected for the hollow cathode effect, since the larger the inter-cathode distance, the higher is the time to obtain similar texture surfaces.

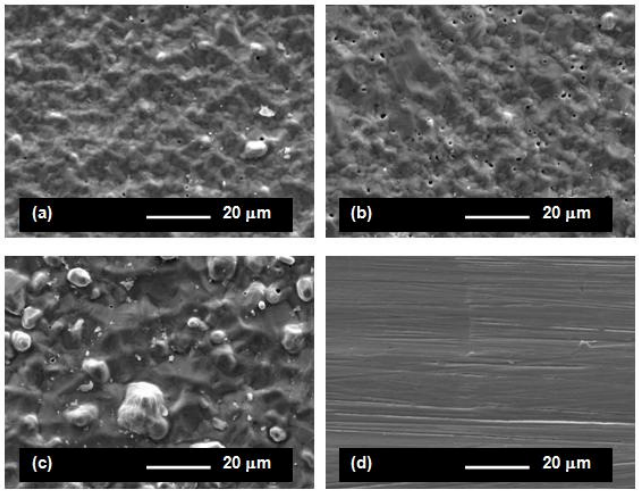

Figure 6. Surface finish aspects of the internal surface of the external cathodes processed in HCD for inter-cathode distance of: a) 3.2 mm; b) 5.8 mm; c) 9.2 mm; and d) in the as non-processed condition.

Results in Fig. 6 indicate that the obtainment of a texture surface is related to the inter-cathode distance parameter. For smaller inter-cathode distances (3.2 and 5.8 mm, Figs. 6a and 6b, respectively) the surface morphology is changed, since the texture of particle observed for the larger inter-cathode distance disappeared (in relation to a = 9.2 mm, Fig. 6c). Furthermore, for inter-cathode distances of 3.2 and 5.8 mm (Fig. 6a and 6b, respectively) another characteristic tends to be present at surface, since nanometric and micrometric porosity appears. This fact is probably related to the presence of argon atoms from the gaseous mixture dissolved into surface (see Table 1). In such case, the intense ion bombardment effect would tend to increase the point crystalline defects, and an increment in the vacancy density could be expected. The argon atom-vacancy pair diffusion could result in the coalescence of them at surface, leading to the formation of new and small porous. It is important emphasizing this event would allow describing a new kind of surface texturing, which could be useful to store liquid lubricants and present beneficial effects of surface texturing, as that verified on mixed lubricated contacts, in accordance with Krupka et al. (2008) study.

According to the chemical analysis of the internal surface of the external cathodes (Table 1), the increase in the Fe contents and consequent decreasing in the amount of Cr, Ni, Si and Mn indicates that the Fe atoms sputtered from the pressed iron samples (see results discussed in Fig. 3) diffuse into the plasma and condense on the internal surface of the external cathode. It is to be noted a strong increment in the amount of iron atoms altering the chemical composition of the surrounding surface as the inter-cathode distance decreases (5.8 at.% Fe and 7.3 at.% Fe, as the inter-cathode distance is changed from a = 9.2 to a = 5.8 mm, and from a = 5.8 to a = 3.2 mm, respectively). The above-mentioned results are in agreement with the expected for the hollow cathode effect, the mass loss verified in Fig. 4, and the results presented in the Part I. Note that the higher hollow cathode effect occurring to the 3.2 mm inter-cathode distance implied necessarily in the decrease of the ton utilized to reach 1423 K (1150 °C) sintering temperature, as seen in the experimental procedure, which could explain the reduced occurrence of the re-sputtering phenomenon in the present study. It is interesting to observe similar results were obtained for the iron concentration in the a = 9.2 mm and 120 min sintering time condition, and a = 5.8 mm and 30 min sintering time (as previously presented in Part I), which was of 71.4 at.% Fe and 71.6 at.% Fe,

respectively. The same was roughly verified in the a = 3.2 mm and 120 min sintering time condition, and a = 5.8 mm and 240 min sintering time (as previously presented in Part I), being of 84.5 at.% Fe and 81.1 at.% Fe, respectively. Finally, the presence of argon in the composition of the processed surfaces is indicative that ions participate in the formation process of the condensed particles, in accordance with the proposed by Romanowsky and Wronikowsky (1992).

Table 1. Average concentrations and standard deviation of Cr, Ni, Si, Fe and Ar measured on the internal surface of the external cathodes processed with different inter-cathode distances (Manganese was not met).

Inter-cathode distance (mm)	Chromium (at.%)	Nickel (at.%)	Silicon (at.%)	Iron (at.%)	Argon (at.%)
as non-processed	25.8 + 0.5	16.0 + 0.4	1.5 + 0.1	55.2 + 0.5	0
3.2	9.1 + 2.0	4.1 + 0.4	0.4 + 0.1	84.5 + 1.0	1.9 + 0.2
5.8	14.5 + 1.4	5.7 + 0.7	0.6 + 0.1	77.2 + 1.1	2.0 + 0.1
9.2	18.2 + 0.9	8.4 + 0.7	0.5 + 0.1	71.4 + 1.2	1.5 + 0.3

Figure 7 shows the Ra and Rz roughness measurements of the internal surfaces as a function of the inter-cathode distance, taken to evaluate the surface changes as a consequence of the sputtering effects on the external cathodes. The Ra and Rz values were 0.55, 0.43 and 0.67 µm, and 4.73, 4.5 and 5.47 µm, for inter-cathode distances of 3.2, 5.8 and 9.2 mm, respectively. It is evidenced the Ra and Rz roughness tend to minimum values when the 5.8 mm inter-cathode distance is utilized, which is in accordance with the results discussed in Fig. 6. Considering the different textures obtained for a = 9.2 mm and a = 5.8 mm, results confirm the assumption that the round-particle atoms tend to dissolve into surface, which explains the decrease of the Ra and Rz roughness values. Otherwise, the increase of the Ra and Rz roughness values obtained for a = 3.2 mm, in relation to a = 5.8 mm, could be explained by the hollow cathode effect, which would lead to an increase in the density of the incident ions in both the surfaces in the annular glow discharge, and consequently in the increase of the sputtering effect, along the same sintering time.

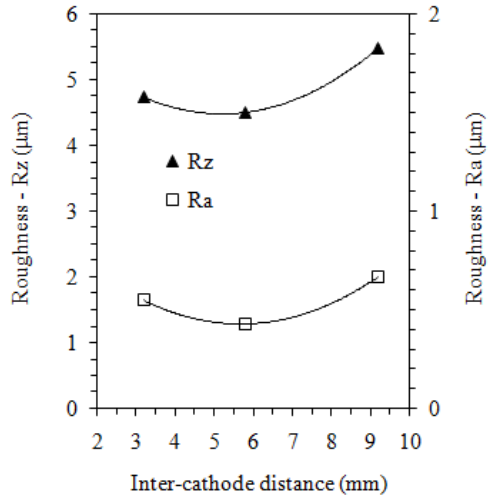

Figure 7. Ra and Rz roughness measurements of the internal surfaces of the external cathodes processed for different inter-cathode distances.

Aspects Related to the Gas Pressure

a) In the Cylindrical Surface of the Iron Samples

Surface finish aspects of the iron samples sintered in HCD are shown in Fig. 8. To emphasize the effects of the ion bombardment on the surface characteristics of the samples, a same place was characterized by SEM before (in the pressed or green state – Fig. 8: a1, b1, c1 and d1) and after plasma exposition (in the sintered state – Fig. 8: a2, b2, c2 and d2), for pressures of 133, 400, 800 and 1200 Pa (1, 3, 6 and 9 Torr), respectively.

Two different aspects can be observed: a) the surface finishing modification; and b) the surface pores' morphology modification. The first aspect is related to the confrontation of the results shown in the Fig. 8 (a2, b2, c2, d2), which indicates the modification of the surface finishing is strongly dependent on the pressure.

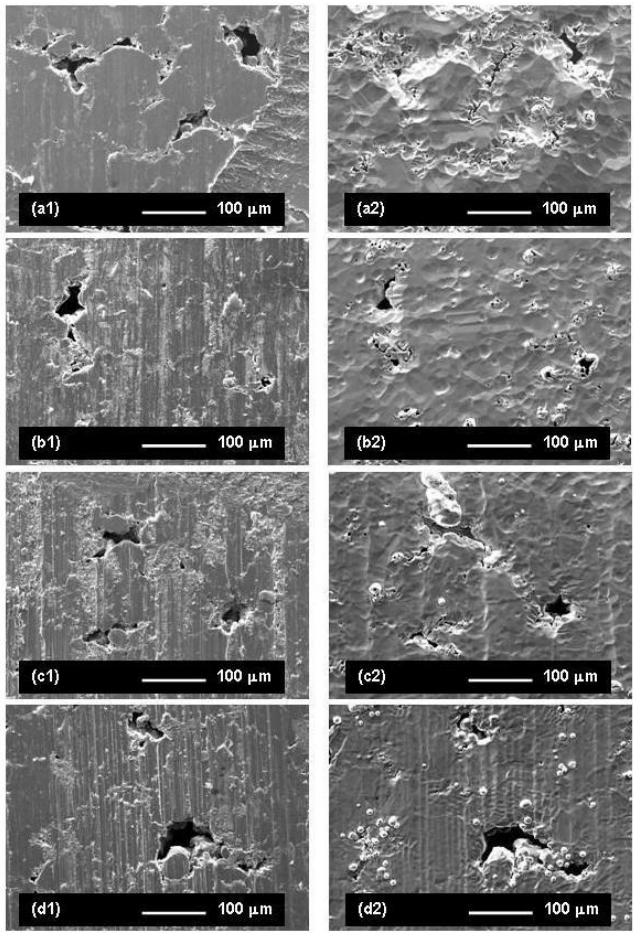

Figure 8. Surface finishing aspects of the iron samples: a1, b1, c1 and d1) in the pressed state; and a2, b2, c2 and d2) after plasma exposition, for pressures of 133, 400, 800 and 1200 Pa (1, 3, 6 and 9 Torr), respectively.

For lower pressures (133 and 400 Pa, or 1 and 3 Torr, respectively), strong alteration in surface finishing is verified (see Fig 8: a2, b2). The changes in the surface finishing can be explained

by the intense sputtering mechanism caused by ion bombardment phenomenon on the surfaces exposed to the plasma in the HCD, resulting in the sputtering of iron atoms from the sample surface. Otherwise, as shown in Fig. 8 (c2, d2), it is also evidenced the start surface is practically maintained for higher pressures (800 and 1200 Pa, or 6 and 9 Torr, respectively). In the case of the use of higher pressures, the mean free path is too much reduced, which increases the backscattering effect, leading the iron atoms sputtered from the sample surface to re-condense on the primitive surface. As an example, it is interesting to observe for the 9 Torr processed sample, the morphology of the initial surface (Fig. 8: d1) is maintained with slight modifications, since the scratches obtained when the pressed sample was extracted from the die remained unaltered after plasma exposition (Fig. 8: d2).

Figure 9 shows the mass loss measurements of the samples, taken to evaluate the sputtering effect on the central cathode. The mass losses were 0.55, 0.46, 0.20 and 0.13% (27.5, 23.2, 9.8 and 6.5 mg), for pressures of 133, 400, 800 and 1200 Pa (1, 3, 6 and 9 Torr), respectively, confirming the relation of the sputtering effect on the sample surfaces' characteristics as a function of the pressure, as observed in Fig. 8. It is evidenced that for 1200 Pa (9 Torr) pressure the mass loss tends to a minimum value, and for 133 Pa (1 Torr) pressure the mass loss tends to a maximum value.

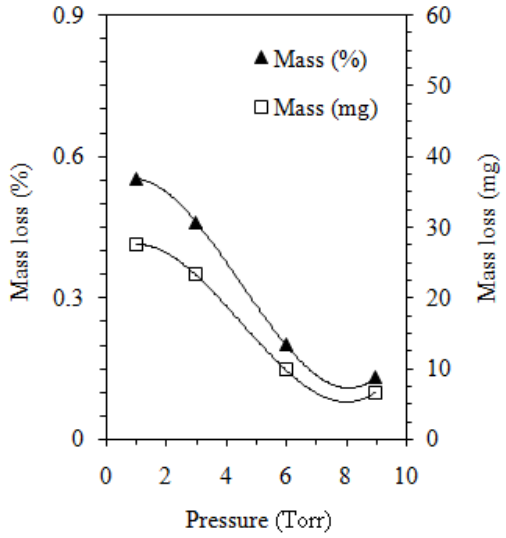

Figure 9. Mass loss measurements of the iron samples processed for different pressures.

Figure 10 shows Ra and Rz roughness measurements of the samples, taken to evaluate the surface changes as a consequence of the sputtering effects on the central cathode, according to the pressure. The Ra and Rz were 0.51, 0.39, 0.31 and 0.23 µm and 2.3, 2.1, 1.5 and 1.2 µm, for pressures of 133, 400, 800 and 1200 Pa (1, 3, 6 and 9 Torr), respectively, confirming the enhancement of the surface modification as the pressure is decreased, which agrees with the previously shown in Fig. 8 (a2, b2, c2, d2).

The second aspect is related to the confrontation of the results shown in Fig. 8 (a1 x a2, b1 x b2, c1 x c2, d1 x d2). It is important to note that the sputtering effect tends to promote significant changes on the superficial pores' morphology, which depend on the pressure and the start size of the pores in the pressed samples cylindrical surfaces. Note that strong changes in the open pore's apparent volume can be observed for the lower treatment pressures (133 and 400 Pa, or 1 and 3 Torr, respectively), as verified in Fig. 8 (a1 x a2, b1 x b2). Otherwise, slight changes in the open pore apparent volume were observed for the higher treatment pressures (800 and 1200 Pa, or 6 and 9 Torr, respectively), as shown in Fig. 8 (c1 x c2, d1 x d2). In addition, the results shown in Fig. 8 clearly indicate the open pores tend to became closed as a consequence of the intense material transport mechanism verified for the metallic atoms, by the interactions in plasma-surface system, for pressure conditions which lead to large mean free path and, consequently, to decrease of the backscattered effect. In such case, higher is the probability of a metallic atom sputtered from the sample to reach the surrounding surface. So, a tendency of surface modification in the pore size distribution could be expected by decrease of the pressure, which would lead to a fine and disperse distribution of small open pores, in accordance with the results shown in Fig. 8 (a1 x a2, b1 x b2), considering the parameters studied. The above findings indicate the pressure is an important discharge parameter, when reduction in the surface pore size is desirable. The results also show that the hollow cathode discharge could be applied to develop a new green technology for surface texturing, becoming a new technique to improve surface properties such as roughness and morphology. These properties are important parameters for many applications directly related to the coatings adhesion, tribological performance, and others, in accordance with Gupta et al. (2007), Basnyat et al. (2008), and Krupka et al. (2008).

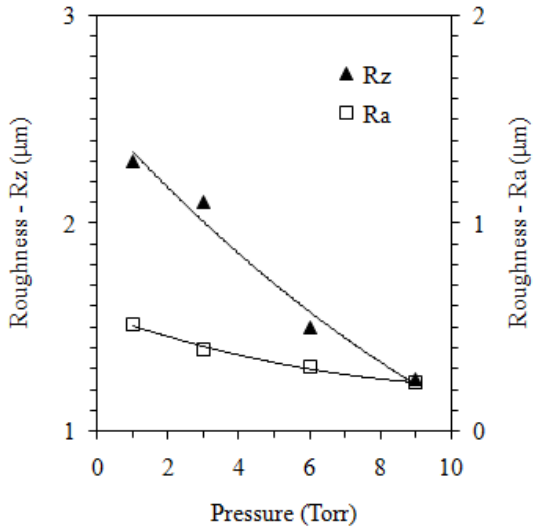

Figure 10. Ra and Rz roughness measurements of the iron samples processed for different pressures.

b) In the Internal Surface of the External Cathodes

Surface finish aspects of the internal surface of the external cathodes processed in HCD are shown in Fig. 11. To emphasize the effects of the sputtering on the characteristics of the internal surface as a function of the pressure, results are compared with the start surface condition (Fig. 11e), which was obtained by polishing. Results indicate that the surface morphology is highly dependent on the pressure. It is evidenced for 1200 Pa (9 Torr) pressure, the morphology comprises revealed grain boundaries, and few and small particles deposited on surface (Fig. 11d). The process of grain boundary's revelation is a consequence of the sputtering caused by the ion bombardment effect on the internal surface of the external cathode. As grain boundaries are regions of discontinuity in the crystalline lattice, metallic atoms placed in these positions are more easily sputtered from the surface. The small amount of particles deposited on the surface is a consequence of the low mass loss

evidenced for the iron sample processed in this condition, as previously discussed. At 800 Pa (6 Torr) pressure, the characteristic twined grain boundaries of the austenite microstructure, which are not evident for the 1200 Pa (9 Torr) pressure processed sample, are revealed with higher definition, and the amount of small particles deposited on surface is increased, as a consequence of the increment of sputtering mechanism (Fig. 11c). Note that the particles growing process was initiated, since the size of the particles deposited was increased, which is in accordance with the higher mass loss evidenced for the processed sample. At 400 Pa (3 Torr) pressure, the particles growing's process is intensified, and a morphology comprised of grown and round particles in a non-homogeneous dispersion is obtained (Fig. 11b), which are probably formed from the deposition of metallic atoms clusters plus ions obtained at plasma phase and subsequent coagulation or sintering on the surface, as previously discussed in the Part I. This assumption is also valid for the particles obtained in Fig. 11(c, d).

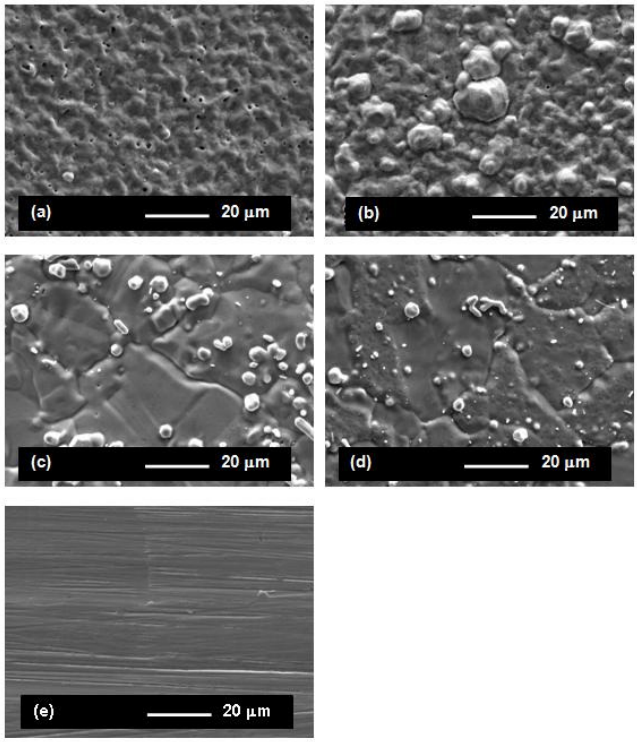

Figure 11. Surface finish aspects of the internal surface of the external cathodes processed in HCD for pressures of: a) 133 Pa (1 Torr); b) 400 Pa (3 Torr); c) 800 Pa (6 Torr); d) 1200 Pa (9 Torr); and e) in the non-processed condition.

Finally, as shown in Fig. 11(a), for the lowest pressure (133 Pa, or 1 Torr), the round particle texture observed for 400 Pa (3 Torr) pressure disappears, indicating the round-particle atoms tend to dissolve into surface as a consequence of the intense hollow cathode effect verified for the related process condition. In addition, another characteristic tends to present at surface, since nanometric and micrometric porosity appears (Fig. 11a). As previously discussed in the inter-cathode distance study, such result could be also related to the presence of argon atoms from the gaseous mixture dissolved into surface as a function of the pressure (see Table 2). In such case, the assumption based on the fact that the intense ion bombardment effect would tend to increase the point crystalline defects and consequently to increment the vacancy density could be also valid here. The argon atom-vacancy pair diffusion could result in the coalescence of them at surface, leading to the formation of new and small porous.

According to the chemical analysis of the internal surface of the external cathodes for different pressures (Table 2), the increase in the Fe contents and consequent decreasing in the amount of alloying elements indicates the Fe atoms sputtered from the pressed iron samples (see results discussed in Fig. 8) diffuse into the plasma and condense on the internal surface of the external cathode. The higher the pressure, the lower is the amount of iron atoms altering the chemical composition of the surrounding surface. It is to be noted that for 1200 Pa (9 Torr) pressure the modification of the chemical composition practically did not occur, being that the metallic component concentrations remained roughly the same. In such case, the iron content measured was 58.5 at.% Fe, which is only 6.0% higher than the verified for the cathode in the start condition (as non-processed). The same mathematical treatment leads to iron contents of 14.8, 37.5 and 46.7% higher than the verified for the cathode in the start condition, for pressures of 800, 400 and 133 Pa (6, 3 and 1 Torr), respectively. These results are in agreement with the mass loss of the sintered iron samples (Fig. 9) and the aspect of the surface morphology obtained, as a function of the pressure (Fig. 11). Otherwise, as discussed by Timanyuk and Tkachenko (1989), the dark space (or the cathode sheath) in the central cathode of an annular discharge is thinner than that observed on the internal surface of the external cathode. In such case, fewer collisions between the plasma species (ions and neutrals) tend to occur in the central cathode sheath than in the internal surface of the external cathode, resulting in a higher kinetic energy of the incident species and, hence, in a higher sputtering yield of the sample surface, which explains the tendency of the internal surface's modification of the external cathodes by iron atoms sputtered from the central cathode, as discussed in this work. It is interesting to observe similar results were roughly verified for the iron concentration in the internal surface of the external cathode after HCD processing for three different conditions, as follows:

a) 81.0 at.% Fe, for p = 133 Pa (1 Torr), a = 5.8 mm and 60 min sintering time;

b) 81.1 at.% Fe, for p = 400 Pa (3 Torr), a = 5.8 mm and 240 min sintering time (as previously presented in Part I); and

c) 84.5 at.% Fe, for p = 400 Pa (3 Torr), a = 3.2 mm and 120 min sintering time (as previously presented here).

By comparing these results, the relation between the hollow cathode effect and its influence on the sputtering effect as a function of the "a x p" product is also evidenced. The first condition above-mentioned presents "a x p" product value of 0.58 cmTorr. As can be observed, the third condition results in "a x p" product value of 0.96 cmTorr, leading to an increase in the sintering time on the order of 60 min in relation to the first condition. And the second condition results in "a x p" product value of 1.74 cmTorr, leading to an increase in the sintering time on the order of 180 min in relation to the first condition.

Finally, it is important to note the presence of argon in the composition of the processed surfaces. As evidenced in Table 2, the higher the pressure, the lower is the argon content retained on the internal surface of the external cathode, which is in accordance with the lower energy of the incident species on the cathode surfaces verified for higher pressures.

Figure 12 shows Ra and Rz roughness measurements of the internal surfaces as a function of the pressure, taken to evaluate the surface changes as a consequence of the sputtering effects on the external cathodes. The Ra and Rz were 0.28, 0.62, 0.93 and 0.58 μm and 2.87, 4.96, 7.40 and 4.80 μm for pressures of 133, 400, 800 and 1200 Pa (1, 3, 6 and 9 Torr), respectively.

Table 2. Average concentrations and standard deviation of Cr, Ni, Si, Fe and Ar measured on the internal surface of the external cathodes processed for different pressures (Manganese was not met).

Pressure (Torr)	Chromium (at.%)	Nickel (at.%)	Silicon (at.%)	Iron (at.%)	Argon (at.%)
as non-processed	25.8 + 0.5	16.0 + 0.4	1.5 + 0.1	55.2 + 0.5	0
1	13.0 + 1.1	4.0 + 0.3	0.4 + 0.1	81.0 + 1.0	1.6 + 0.1
3	14.8 + 1.4	7.3 + 0.6	0.7 + 0.1	75.9 + 1.1	1.3 + 0.1
6	22.3 + 1.7	12.9 + 0.4	0.9 + 0.1	63.4 + 1.1	0.5 + 0.3
9	25.2 + 1.0	14.8 + 0.3	0.9 + 0.1	58.5 + 1.2	0.2 + 0.1

As evidenced in Fig. 9, as the pressure decreases the amount of iron atoms sputtered from the sample is increased. So, the tendency to form particles on the internal surface of the external cathode is also increased (see Fig. 11), saved the 133 Pa (1 Torr) condition. This explains the higher values of Ra and Rz roughness obtained for samples processed in 1200 and 800 Pa (9 and 6 Torr, respectively). Simultaneously to this event, for lower pressures (400 and 133 Pa, or 3 and 1 Torr, respectively), the continuous and more intense ion bombardment effect at these conditions, as discussed above, acts in promoting the diffusion of the particle atoms, which tend to dissolve into surface, explaining the decrease of the Ra and Rz roughness values verified in such cases.

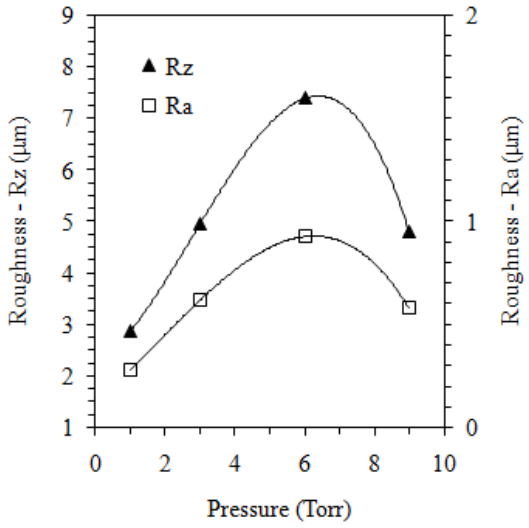

Figure 12. Ra and Rz roughness measurements of the internal surfaces of the external cathodes processed for different pressures.

Conclusion

The influence of the inter-cathode distance and the pressure on the surface morphology's changes in pressed iron samples and in the internal surface of the external cathodes was investigated in HCD.

It was evidenced the hollow cathode effect, which is directly related to the inter-cathode distance, strongly affects the sputtering mechanism. It was also verified sputtering mechanism in HCD promotes significant surface finishing's differences between the pressed and sintered samples, but the effect of the inter-cathode distance was not so evident probably as a consequence of the high sintering time specified for this study. The sputtering effect tends to promote significant reduction in the pore's apparent size in the sintered samples' surface, which was verified for all the inter-cathode distances studied, and the surface finishing aspects, morphology and chemical composition of the internal surface of the external cathodes can be modified as a function of the inter-cathode distance. Finally, it is to be noted that an intermediary inter-cathode distance, in such case on the order of 6 mm, is indicated to achieve adequate heating control in HCD processing, and so in HCD sintering and texturing treatments.

In addition, the results indicate that the sputtering mechanism in HCD sintering and texturing treatments can be adequately controlled as a function of the pressure, comprising an important contribution to the development of green technologies for surface texturing, surface engineering, and for part's sintering. The main conclusions can be listed as follows:

a) Strong modification of the surface finishing, roughness and morphology is evidenced in the sintered samples as a function of the pressure, which makes it possible the obtainment of different surface texturing as, simultaneously, the sintering process runs;

b) As expected, sputtering mechanism is strongly dependent on the pressure parameter and it tends to promote significant changes on the superficial pores' morphology. In such case, the use of a low pressure (on the order of 133 Pa, or 1 Torr) is decisive, when the reduction in the pore apparent size in the sintered samples surface is desirable. Otherwise, the use of a high pressure (on the order of 1200 Pa, or 9 Torr) is decisive when the maintenance of the start surface characteristics are desirable in both the cathodes' surface; and

c) Surface finishing aspects, morphology and chemical composition of the internal surface of the external cathodes can be strongly modified as a function of the pressure.

Acknowledgments

The author would like to thank the Brazilian Agency CNPq for financial support, and the M.Sc. V. Pimentel and M.Sc. J. W. Muller for the roughness profile measurements.

References

Basnyat, P., Luster, B., Muratore, C., Voevodin, A.A., Haasch, R., Zakeri, R., Kohli, P., Aouadi, S.M., 2008, "Surfacing texturing for adaptive solid lubrication". *Surface & Coatings Technology*, Vol. 203, pp. 73-79.

Benda M., Vlcek J., Cibulka V., Musil J., 1997, "Plasma Nitriding Combined With a Hollow Cathode Discharge Sputtering at High Pressures". *J. Vac. Sci. Technol. A*, Vol. 15, n. 5, pp. 2636-2643.

Brunatto, S.F., Khün, I., Muzart, J.L.R., 2001, "Influence of the Radial Spacing between Cathodes on the Surface Composition of Iron Samples Sintered by Hollow Cathode Electric Discharge". *Materials Research*, Vol. 4, n. 4, pp. 245-250.

Brunatto, S.F., Khün, I., Muzart, J.L.R., 2005, "Surface Modification of Iron Sintered in Hollow Cathode Discharge Using an External Stainless Steel Cathode". *J. Phys. D: Appl. Phys.*, Vol. 38, pp. 2198-2203.

Brunatto S.F. and Muzart J.L.R., 2007, "Influence of the gas mixture flow on the processing parameters of hollow cathode discharge iron sintering". *J. Phys. D: Appl. Phys.*, Vol. 40, pp. 3937-3944.

Brunatto, S.F., Klein, A.N., Muzart, J.L.R., 2008, "Hollow Cathode Discharge: Application of a Deposition Treatment in the Iron Sintering", *J. of the Braz. Soc. of Mech. Sci. & Eng.* (ABCM), Vol. XXX, n. 2, pp. 145-151.

Gupta, P., Tenhundfeld, G., Daigle, E.O., Ryabkov, D., 2007, "Electrolytic plasma technology: Science and engineering – An overview". *Surface & Coatings Technology*, v. 201, pp. 8746-8760.

Koch, H. *et al.*, 1991, "Hollow Cathode Discharge Sputtering Device for Uniform Large Area Thin Film Deposition". *J. Vac. Sci. Technol. A*, Vol. 9, n. 4, pp. 2374-2377.

Kolobov, V.I., Tsendin, L.D., 1995, "Analytical Model of the Hollow Cathode Effect". *Plasma Sources Sci. Technol.*, Vol. 4, pp. 551-560.

Krupka, I., Vrbka, M., Hartl, M., 2008, "Effect of surface texturing on mixed lubricated non-conformal contacts". *Tribology International*, Vol. 41, pp. 1063-1073.

Muzart, J.L.R., Batista, V.J., Franco, C.V., Klein, A.N., 1997, "Plasma Sintering of AISI 316L Stainless Steel: The influence of the Processing Cycle on the Sample Density". Proceedings of Advances in Powder Metallurgy & Particulate Materials – MPIF, Part 3, pp. 77-84.

Romanowsky, Z., Wronikowski, M., 1992, "Specific Sintering by Temperature Impulses as a mechanism of Formation of a TiN Layer in the Reactive Pulse Plasma". *Journal of Materials Science*, Vol. 27, pp. 2619-2622.

Timanyuk V.A., Tkachenko V.M., 1989, "Study of a Glow Discharge in an Annular Cathode Cavity". *Sov. Phys. Tech. Phys.*, Vol. 34, n. 7, pp. 832-834.

V. Engel, A., 1994, "Ionized Gases". 2nd ed., American Institute of Physics, New York, USA, p. 325.